

## The interacting galaxy cluster “El Gordo” a massive blow to $\Lambda$ CDM cosmology

---

**Elena Asencio**<sup>1,\*</sup>

<sup>a</sup>*Helmholtz-Institut für Strahlen und Kernphysik (HISKP), University of Bonn,  
Nussallee 14-16, D-53115 Bonn, Germany*

*E-mail:* [s6elena@uni-bonn.de](mailto:s6elena@uni-bonn.de)

El Gordo (ACT-CL J0102-4915) is an extremely massive galaxy cluster ( $2.13_{-0.23}^{+0.25} \times 10^{15} M_{\odot}$ ) at redshift  $z=0.87$ , composed of two interacting subclusters with mass ratio 1.52. Hydrodynamical simulations of the interaction suggest that  $V_{\text{infall}} \approx 3000$  km/s is required to match the observed luminosity and morphology of El Gordo. In this work, we determine the probability of finding a similar object – in terms of total mass, mass ratio, redshift, and infall velocity – in a  $\Lambda$ CDM context using the cosmological simulation "Jubilee". We find that the probability of detecting at least one candidate in the simulation box is of  $7.33 \times 10^{-8}$  (i.e, El Gordo is in  $5.38\sigma$  tension with the model). The probability decreases to  $1.06 \times 10^{-8}$  ( $5.72\sigma$  tension) when also taking into account the Bullet Cluster. These systems arise naturally in a Milgromian dynamics (MOND) cosmology with light sterile neutrinos.

*Corfu Summer Institute 2022 "School and Workshops on Elementary Particle Physics and Gravity",  
28 August - 1 October, 2022  
Corfu, Greece*

---

\*Speaker

## 1. Introduction

According to the current standard model of cosmology ( $\Lambda$ CDM) [1], structures in the Universe formed in a hierarchical way [2]. That is, smaller structures formed first and then, by accretion and mergers, they came together to form larger structures. The largest structures in the Universe which are held together by their own gravity are the galaxy clusters. The redshift ( $z$ ) at which these structures are observed can be compared with their predicted formation time scale, which depends on the cosmological model adopted. This makes them valuable probes to check the applicability of cosmological models.

In the last years, there have been significant improvements on the capability of the telescopes to look deeper into space. This has made possible the detection and the analysis of more distant objects. Recent surveys have already found several objects whose mass, redshift and/or infall velocity are unusually high, according to  $\Lambda$ CDM expectations (e.g. the Bullet Cluster [3], PLCK G287.0+32.9 [4], SPT-CL J2106-5844 [5], etc.). A particularly extreme example of this is the galaxy cluster ACT-CL J0102-4915, also known as “El Gordo”.

El Gordo is a supermassive interacting galaxy cluster observed at redshift  $z = 0.87$ . It was found by the Atacama Cosmology Telescope (ACT) collaboration in a 455 deg<sup>2</sup> survey [6, 7]. It has a total mass of  $M_{200} = 2.13^{+0.25}_{-0.23} \times 10^{15} M_{\odot}$  and is composed of two infalling subclusters with mass ratio 1.52. When the mass of each subcluster is obtained individually, the total mass of El Gordo is slightly lower  $M_{200} = 1.64^{+0.40}_{-0.36} \times 10^{15} M_{\odot}$  [8].

The properties of El Gordo were constrained for the first time by [9] from the analysis of multiwavelength observations. Their results indicated that this galaxy cluster presents a very high X-ray luminosity and a strong Sunyaev-Zel’dovich (SZ) effect, from which a high collision velocity can be inferred. They also noted the presence of a wake formed in the X-ray surface brightness caused by the passage of one subcluster through the other.

Several studies had already pointed out that the properties of El Gordo are quite rare in the context of  $\Lambda$ CDM [9–11]. In this study we quantify with a detailed analysis the likelihood of observing an object with the mass, infall velocity and redshift of El Gordo in a  $\Lambda$ CDM cosmology – considering the mass and mass ratio values given by the latest observations on this cluster [8].

In Section 2 the method followed throughout the study is described, as well as the properties of the cosmological simulation and the hydrodynamical simulations considered for the analysis; in Section 3 the statistical analysis used to find the likelihood of observing a El Gordo-like object is described; the results are shown in Section 4 and, finally, in Section 5, the conclusions are presented.

## 2. Method

In order to find out the number of El Gordo-like objects that one should expect in a  $\Lambda$ CDM cosmology, one can use cosmological simulations. These simulations are very useful for understanding the properties of the objects that formed at a certain redshift, according to a certain model. However, they do not have enough resolution to reproduce some of the more detailed features of these objects (e.g. the two-tailed X-ray morphology of El Gordo can not be reproduced in a cosmological simulation). Still, it is possible to find objects whose properties could potentially give rise to these features. That is, objects with properties that are analogous to those of the El

Gordo progenitors. Hydrodynamical simulations are needed in order to find out what properties of mass, mass ratio and infall velocity are needed for the progenitor clusters to reproduce the observed morphology of El Gordo (as well as its luminosity and temperature). The cosmological simulation and the hydrodynamical simulation used to search for analogues of the El Gordo progenitors and to constrain their properties, respectively, are briefly described below.

## 2.1 The cosmological simulation Juropa Hubble Volume (Jubilee)

The Juropa Hubble Volume (Jubilee) [12] simulation is a N-body  $\Lambda$ CDM simulation based on the Wilkinson Microwave Anisotropy Probe (WMAP) results [13], which constrained the following values for the cosmological parameters:  $\Omega_{m,0} = 0.27$ ,  $\Omega_{\Lambda,0} = 0.73$ ,  $h = 0.7$ ,  $\sigma_8 = 0.8$ ,  $n_s = 0.96$ ,  $\Omega_{b,0} = 0.044$ . The simulation is post-processed with the halo identifier Amiga Halo Finder (AHF) [14, 15], and is available at redshifts  $z = 0$ ,  $z = 0.509$ ,  $z = 1$ , and  $z = 6$ . The lowest halo mass is composed of 20 particles, each particle having mass of  $7.49 \times 10^{10} h^{-1} M_{\odot}$ . For this project, their largest volume box  $(6h^{-1} \text{ cGpc})^3$  was used.

## 2.2 The hydrodynamical simulations

Hydrodynamical simulations are needed to understand the gas dynamics required to reproduce the temperature, luminosity and morphology of El Gordo. The latest and most complete exploration of the El Gordo parameter space using hydrodynamical simulations was done by [16]. This is also the simulation that better reproduces the observed properties of El Gordo. [16] tested two different scenarios for the interaction. The first scenario (referred to as Model A by the authors) assumed that the interaction is a very energetic head-on collision between the two subclusters. The best-fit parameters found by [16] in their Model A are:  $M_{200} = 1.95 \times 10^{15} M_{\odot}$ , mass ratio of 2, and infall velocity  $V_{\text{infall}} = 3000 \text{ km/s}$  when the subclusters are at twice the sum of their virial radii from each other. With these parameters, they could generate X-ray surface brightness and mass density distributions that match the observations. But the twin-tailed X-ray morphology that they obtained was smaller and more asymmetric than observed, and only appeared when the projected distance between the clusters was  $\approx 600 \text{ kpc}$  ( $\approx 100 \text{ kpc}$  smaller than observed).

In their second scenario (Model B), [16] assumed that the interaction took place as a less violent, off-centred collision. The best-fit parameters in the Model B case are:  $M_{200} = 3.19 \times 10^{15} M_{\odot}$ , mass ratio of 3.6, and  $V_{\text{infall}} = 2500 \text{ km/s}$  at twice the sum of the virial radii of the subclusters. With these parameters, the model reproduced the temperature and X-ray luminosity of El Gordo and a two-tailed X-ray morphology that looked more similar to the observed one, in terms of the size and symmetry of the tails. The projected separation of the simulated subclusters is also closer to the observed one ( $\approx 780 \text{ kpc}$ ).

Even though the fiducial Model B of [16] manages to reproduce the properties of El Gordo better than their Model A, the mass and mass ratio parameters used in Model A are closer to the values found by the latest observational studies on the El Gordo mass [8]. Therefore,  $V_{\text{infall}} = 3000 \text{ km/s}$  – as constrained in Model A – is considered in the following analysis as the expected infall velocity of the El Gordo progenitors.

### 3. Statistical analysis

In order to find the probability of observing an El Gordo-like object in a  $\Lambda$ CDM cosmology, analogues to the El Gordo progenitors are searched for in the Jubilee simulation box. The conditions that a pair of halos must fulfill in order to be considered candidates are the following:

1. They must be at  $z \geq 1$ , since the aim is to find a configuration prior to the observed one ( $z = 0.87$ ) in which the subclusters have not yet interacted.
2. They must have turned around from cosmic expansion. That is, the subclusters must potentially be able to fall into each other and, for this, it is required that the scale product of their velocity and distance vectors is smaller than 0:  $\mathbf{v} \cdot \mathbf{r} < 0$
3. Their mass ratio must be smaller or equal to the mass ratio expected for the El Gordo progenitors: mass ratio  $\leq 1.52$  [8].
4. The ratio  $\tilde{v}$  between the infall velocity and the escape velocity at twice the sum of the virial radii of the subclusters must be higher or equal to the  $\tilde{v}$  expected for the El Gordo progenitors ( $\tilde{v}_{EG}$ ), assuming  $V_{\text{infall}} = 3000$  km/s for them [16]:  $\tilde{v} \geq \tilde{v}_{EG} = 1.88$
5. The total virial mass must be higher or equal to the estimated virial mass of El Gordo ( $M_{200,EG}$ ). In order to be as conservative as possible, the lowest mass estimate allowed within uncertainties in [8] is considered for this analysis:  $M_{200} \geq M_{200,EG} = 1.64 \times 10^{15} M_{\odot}$ . In logarithmic scale this corresponds to:  $\tilde{M} = \log_{10}(M/M_{\odot}) \geq \tilde{M}_{EG} = 15.21$ .

El Gordo is such a massive galaxy cluster that, when the total virial mass condition is imposed, the simulation box runs out of analogues. For a certain redshift, the number ( $N$ ) of El Gordo analogues with the expected total mass can still be inferred by plotting the cumulative mass distribution function of the pairs that match the other conditions (in logarithmic scale) and applying a quadratic fit to the distribution:

$$\log_{10} N(\geq \tilde{M}) = c_0 + c_1 \tilde{M} + c_2 \tilde{M}^2, \quad (1)$$

which can then be extended to  $\tilde{M}_{EG}$ . This distribution and the quadratic fit are shown in Fig.1 for the simulation snapshot at  $z=1$ . Fig.1 also shows the mass distribution of analogues when the  $\tilde{v}$  condition is relaxed to  $\tilde{v} > 0$ .

The value of the coefficients  $c_0$ ,  $c_1$ , and  $c_2$  in Eq.1 varies for each redshift (or scale factor  $a = 1/(1+z)$ ) at which the cumulative mass distribution is fitted. To infer the value for each of these coefficients at any  $a$ , the cumulative mass distribution is fitted in the  $z = 0$ ,  $z = 0.509$ , and  $z = 1$  snapshots in the Jubilee simulation. This provides three different values for each coefficient, which can then be fitted by a quadratic function (in logarithmic scale). With this, it is possible to reformulate Eq.1 as:

$$\log_{10} N(\geq \tilde{M}) = c_0(a) + c_1(a) \tilde{M} + c_2(a) \tilde{M}^2. \quad (2)$$

Then, the number of analogues found in the Jubilee box volume ( $6.3 \times 10^{11}$  cMpc<sup>3</sup>) at any mass and  $a$  is scaled to the survey volume in which El Gordo was originally observed ( $\approx 4 \times 10^8$  cMpc<sup>3</sup>).

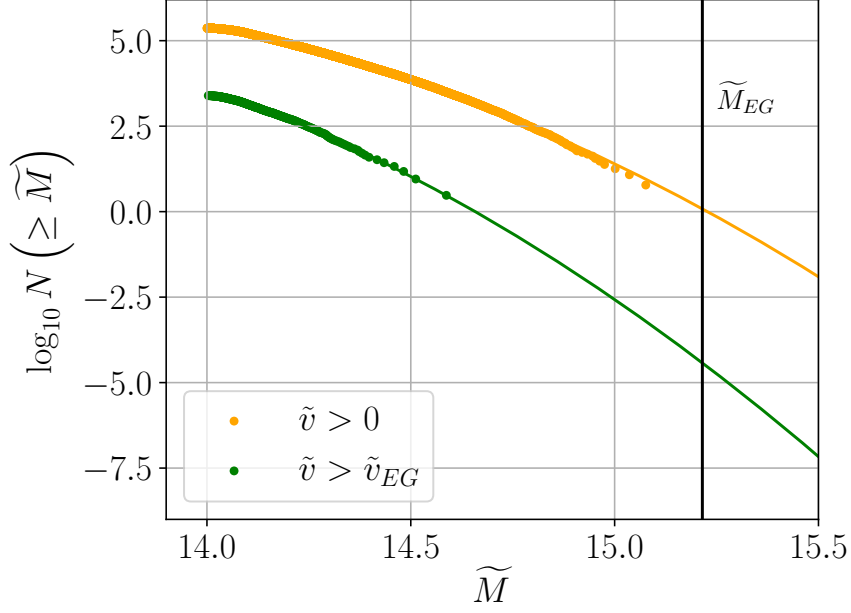


**Figure 1:** Cumulative mass distribution function of the candidate pairs in the  $z = 1$  simulation box. These pairs match the turn around and the mass ratio  $\leq 1.52$  conditions. The orange points match the additional condition  $\tilde{v} > 0$ , and the green points match the  $\tilde{v} > \tilde{v}_{EG}$  condition, for  $\tilde{M}_{EG} = 15.21$  and  $\tilde{v}_{EG} = 1.88$ . Both distributions are fitted with a quadratic function. The black vertical line indicates the assumed total mass (in logarithmic scale and solar mass units) for the pair of El Gordo subclusters [8].

Fig.2 shows a grid of  $a$  and  $\tilde{M}$  values where the corresponding number of analogues in each pixel is represented with a color gradient.

The number of analogues with  $M$  and  $a$  in a less likely region of parameter space than El Gordo progenitors is then converted to a probability using Poisson statistics:  $P = 1 - \exp(-N)$ . This probability can be related to the number of standard deviations by the Gaussian equation:  $1 - \frac{1}{\sqrt{2\pi}} \int_{-\chi}^{\chi} \exp(-x^2/2) dx \equiv P$ .

As mentioned in Section 1, El Gordo is not the only problematic object for  $\Lambda$ CDM. The Bullet cluster is well-known for its unusually high infall velocity, estimated in 3000 km/s [17]. The combined tension between the Bullet Cluster and El Gordo can be obtained approximately by adding the square of the El Gordo  $\chi$  value ( $\chi_{EG}$ ) to  $\chi_{BC}^2$ .

#### 4. Results

Following the method described Section 3, the inferred probability of finding an El Gordo-like object in the survey volume in which El Gordo was observed is  $1.07 \times 10^{-6}$  ( $4.88\sigma$ ), for the conservative mass estimate  $M_{200} = 1.64 \times 10^{15} M_{\odot}$ , and the infall velocity inferred from the hydrodynamical simulations of [16]  $V_{\text{infall}} = 3000$  km/s. It is worth noting that the mass considered in the analysis is the one obtained when each of the subcluster’s mass is measured individually, however, their joint fit should be more representative of the total mass of the cluster, as both clusters

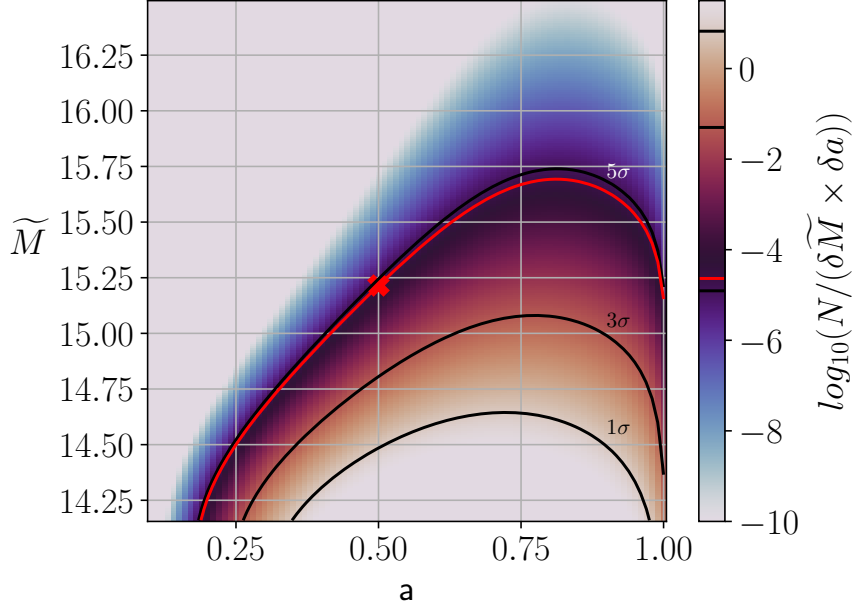


**Figure 2:** Contour plot of the number of analogues expected to be found in the El Gordo survey volume, as a function of the scale factor  $a$  and the mass  $\tilde{M}$  in logarithmic scale and solar mass units. The number of analogues, represented with the color gradient, is scaled by the pixel area  $\delta\tilde{M} \times \delta a = 10^{-4}$  and expressed in logarithmic scale. The black lines represent the contour lines corresponding to  $1\sigma$ ,  $3\sigma$ , and  $5\sigma$  levels. The red cross marks the pixel corresponding to the  $\tilde{M}$  and  $a$  expected for the progenitors of El Gordo. The red line is the contour level that corresponds to the probability of observing an analogue in the survey volume.

are considered simultaneously in the weak lensing analysis. When considering the nominal value for the joint mass fit  $M_{200} = 2.13 \times 10^{15} M_{\odot}$ , the probability decreases to  $7.33 \times 10^{-8}$  ( $5.38\sigma$ ).

[18] found that only 0.1 systems similar to the Bullet Cluster can be expected within  $z < 0.3$  in the whole sky, assuming a  $\Lambda$ CDM cosmology. However, the survey in which the Bullet Cluster was found only covered 5.4% of the sky. When accounting for the size of the survey region, the probability of observing a Bullet Cluster-like object is  $5.4 \times 10^{-3}$  ( $2.78\sigma$ ).

The combined tension between the El Gordo and the Bullet Cluster (obtained as described in Section 3) amounts to  $5.26\sigma$  when assuming  $M_{200} = 1.64 \times 10^{15} M_{\odot}$ . For the joint mass fit  $M_{200} = 2.13 \times 10^{15} M_{\odot}$ , the tension increases to  $5.72\sigma$ .

From this, it can be concluded that the  $\Lambda$ CDM model is rejected with a confidence  $> 5\sigma$ . Other cosmological models have also attempted to reproduce this extreme objects. An example of this is the Neutrino ( $\nu$ ) Hot Dark Matter model ( $\nu$ HDM) [19]. This model assumes sterile neutrinos (instead of the  $\Lambda$ CDM cold dark matter) and Milgromian gravity [20]. With this model, [10] found about one El Gordo analogue in their simulation box. Therefore, it can be relevant to further explore models like  $\nu$ HDM as possible alternatives to the current standard model.

## 5. Conclusions

Assuming the model parameters from [8] and [16], the El Gordo galaxy cluster contradicts the  $\Lambda$ CDM model at  $4.88\sigma$ , even when assuming a conservative mass estimate. For the nominal mass estimate, the tension rises to  $5.38\sigma$ . It should also be taken into account that, besides of El Gordo, there are other problematic objects for the  $\Lambda$ CDM model in the sky. One of the most well-known examples is the galaxy cluster known as the Bullet Cluster. The high infall velocity inferred for its two subclusters makes this object a  $2.78\sigma$  outlier in the  $\Lambda$ CDM model – when scaling the result of [18] to the sky area in which the Bullet Cluster was discovered. Observing both El Gordo and the Bullet Cluster in their respective survey areas yields a combined tension of  $5.26\sigma$  ( $5.72\sigma$  for the nominal mass of El Gordo). It can therefore be concluded that the observations of these extreme objects pose an important challenge to  $\Lambda$ CDM cosmology. The existence of these objects is more plausible in alternative models such as the  $\nu$ HDM cosmology [10, 21].

## Data availability

The data underlying this article are available in the article.

## Acknowledgments

EA is supported by a stipend from the Stellar Populations and Dynamics Research Group at the University of Bonn.

## References

- [1] J.P. Ostriker and P.J. Steinhardt, *The observational case for a low-density Universe with a non-zero cosmological constant*, *Nature* **377** (1995) 600.
- [2] M. Davis, G. Efstathiou, C.S. Frenk and S.D.M. White, *The evolution of large-scale structure in a universe dominated by cold dark matter*, **292** (1985) 371.
- [3] M. Markevitch, A.H. Gonzalez, D. Clowe, A. Vikhlinin, W. Forman, C. Jones et al., *Direct constraints on the dark matter self-interaction cross-section from the merging galaxy cluster 1E 0657–56*, *ApJ* **606** (2004) 819–824.
- [4] Planck Collaboration VI, *Planck intermediate results. VI. The dynamical structure of PLCKG214.6+37.0, a Planck discovered triple system of galaxy clusters*, **550** (2013) A132 [1207.4009].
- [5] R.J. Foley, K. Andersson, G. Bazin, T. de Haan, J. Ruel, P.A.R. Ade et al., *Discovery and cosmological implications of SPT-CL J2106-5844, the most massive known cluster at  $z>1$* , *ApJ* **731** (2011) 86.
- [6] F. Menanteau, J. González, J. Juin, T.A. Marriage, E.D. Reese, V. Acquaviva et al., *The Atacama cosmology telescope: Physical properties and purity of a galaxy cluster sample selected via the Sunyaev-Zel’dovich effect*, *ApJ* **723** (2010) 1523.

- [7] T.A. Marriage, V. Acquaviva, P.A.R. Ade, P. Aguirre, M. Amiri, J.W. Appel et al., *The Atacama Cosmology Telescope: Sunyaev-Zel’dovich-Selected Galaxy Clusters at 148 GHz in the 2008 Survey*, **737** (2011) 61 [[1010.1065](#)].
- [8] J. Kim, M.J. Jee, J.P. Hughes, M. Yoon, K. HyeonHan, F. Menanteau et al., *Head-to-Toe Measurement of El Gordo: Improved Analysis of the Galaxy Cluster ACT-CL J0102-4915 with New Wide-field Hubble Space Telescope Imaging Data*, **923** (2021) 101 [[2106.00031](#)].
- [9] F. Menanteau, J.P. Hughes, C. Sifón, M. Hilton, J. González, L. Infante et al., *The Atacama Cosmology Telescope: ACT-CL J0102-4915 “El Gordo,” a Massive Merging Cluster at Redshift 0.87*, *ApJ* **748** (2012) 7 [[1109.0953](#)].
- [10] H. Katz, S. McGaugh, P. Teuben and G.W. Angus, *Galaxy cluster bulk flows and collision velocities in QUMOND*, *ApJ* **772** (2013) 10.
- [11] M.J. Jee, J.P. Hughes, F. Menanteau, C. Sifón, R. Mandelbaum, L.F. Barrientos et al., *Weighing “El Gordo” with a Precision Scale: Hubble Space Telescope Weak-lensing Analysis of the Merging Galaxy Cluster ACT-CL J0102-4915 at  $z = 0.87$* , **785** (2014) 20 [[1309.5097](#)].
- [12] W.A. Watson, I.T. Iliev, A. D’Aloisio, A. Knebe, P.R. Shapiro and G. Yepes, *The halo mass function through the cosmic ages*, **433** (2013) 1230 [[1212.0095](#)].
- [13] J. Dunkley, E. Komatsu, M.R.olta, D.N. Spergel, D. Larson, G. Hinshaw et al., *Five-Year Wilkinson Microwave Anisotropy Probe Observations: Likelihoods and Parameters from the WMAP Data*, **180** (2009) 306 [[0803.0586](#)].
- [14] S.P.D. Gill, A. Knebe and B.K. Gibson, *The evolution of substructure - I. A new identification method*, *MNRAS* **351** (2004) 399 [[astro-ph/0404258](#)].
- [15] S.R. Knollmann and A. Knebe, *AHF: Amiga’s Halo Finder*, *ApJS* **182** (2009) 608.
- [16] C. Zhang, Q. Yu and Y. Lu, *Simulation the galaxy cluster “El Gordo” and identifying the merger configuration*, *ApJ* **813** (2015) 129.
- [17] C. Lage and G. Farrar, *Constrained simulation of The Bullet Cluster*, *ApJ* **787** (2014) 144.
- [18] D. Kraljic and S. Sarkar, *How rare is the Bullet Cluster (in a  $\Lambda$ CDM universe)?*, *JCAP* **2015** (2015) 050.
- [19] G.W. Angus, *Is an 11 eV sterile neutrino consistent with clusters, the cosmic microwave background and modified Newtonian dynamics?*, *MNRAS* **394** (2009) 527.
- [20] M. Milgrom, *A modification of the Newtonian Dynamics as a possible alternative to the hidden mass hypothesis*, *ApJ* **270** (1983) 365.
- [21] M. Haslbauer, I. Banik and P. Kroupa, *The KBC void and Hubble tension contradict  $\Lambda$ CDM on a Gpc scale – Milgromian dynamics as a possible solution*, **499** (2020) 2845 [[2009.11292](#)].